

Control Strategy of a Power Line Conditioner for Cogeneration Plants

D. Casadei, G. Grandi

Department of Electrical Engineering
University of Bologna
Viale Risorgimento 2, Bologna I-40136

R.K. Jordan

Department of Automation
Technical University of Budapest
Budafoki 8, Budapest H-1111

F. Profumo

Department of Electrical Engineering
Politecnico of Turin
C.so Duca Abruzzi 24, Torino I-10129

Abstract — The cogeneration system analyzed in this paper consists of a high speed turbine coupled to a synchronous generator, that is connected to the mains by an AC/AC power converter. A novel control strategy is proposed for the power conditioning system to provide not only the active power, but the reactive power as well. In this way, the system can be efficiently used for power factor correction and current harmonics compensation. The theoretical analysis is confirmed by computer simulations carried out by PSpice for various operating conditions.

I. INTRODUCTION

In industrial plants and gas networks it is frequently required to reduce the pressure of the steam or some other working medium to a lower value. The pressure reduction is carried out, in most cases, by using special pressure reducing valves. Examples of applications where pressure reduction is frequently needed are chemical and food processing plants and hospitals where the low pressure steam is used for sterilization besides central heating. Theoretically the process of pressure reduction is associated with a loss of entropy that can be saved, by turbines specially designed, to obtain mechanical energy that can further be converted into electric energy by a generator.

A special feature of turbines working at low pressure is the need of high operational speed [1]-[3]. As a consequence, high-speed, permanent-magnet, three-phase synchronous generators, directly connected to the turbine shaft can be an attractive solution. The produced electric

energy can be fed back into the mains by an AC/AC power converter. The converter system is realized by a three-phase diode rectifier supplying the DC-link and a Voltage Source Inverter (VSI) connected to the mains. The parallel connection to the mains is realized through three AC-link inductors.

The basic question determining the applicability of this type of systems is the pay back time of the investment. Some preliminary studies have shown that the pay back time calculated from the investment cost and the price of the electric energy can be relatively short, particularly in countries with high price of electric energy.

The idea presented in this paper makes it possible to improve the likelihood of economical applications by cutting the pay back time, without significantly increasing the investment cost. In particular, a novel control algorithm for the Power Conditioning System (PCS) is proposed, which allows the PCS to behave as an active filter, i.e. to compensate the reactive power and the current harmonics of non-linear loads connected to the same grid [4]-[12].

First the complete system has been simulated in steady-state conditions adjusting all the parameters to achieve, at the rated speed, the rated power. Then, the load has been switched on and switched off, and the perturbation caused in the cogeneration system has been analyzed.

The performance of the control system has been tested also in the case of non-linear loads. The results obtained show that the proposed controller can operate correctly, keeping the generated power close to its reference value. In addition, the source currents are nearly sinusoidal with unity input power factor.

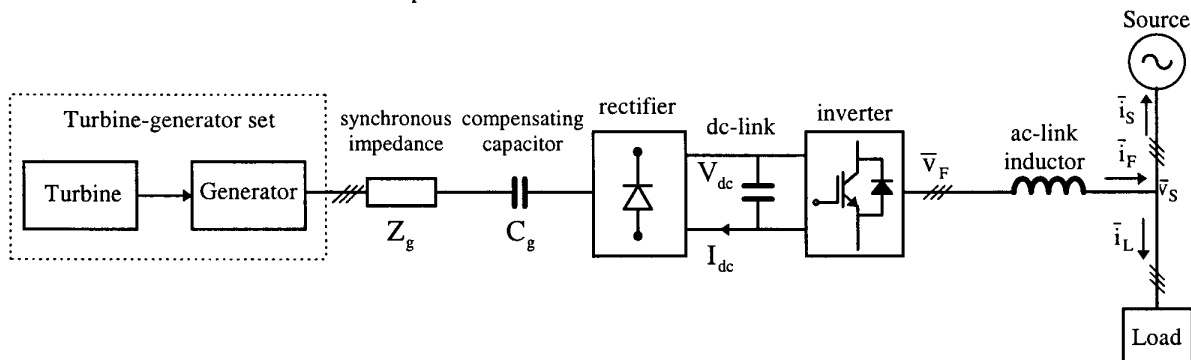


Fig. 1. Block diagram of the cogeneration system.

II. DESCRIPTION OF THE COGENERATION SYSTEM

A simplified block diagram of the whole system is shown in Fig. 1. The three-phase generator operates at 400 Hz, corresponding to the mechanical speed of 12,000 rpm.

The operation of the system is based on two independent control loops, which keep the outlet steam pressure and the intermediate DC-link voltage close to their reference values. An indirect control of the speed is also achieved, being the DC-link voltage proportional to the mechanical speed.

As a result of using rare-earth PM, the armature reaction effect in the generator is quite low, thus the synchronous inductance of the machine is reduced as compared to that of machines with traditional construction. However, due to the high stator frequency the synchronous reactance is still high. Thus, a compensation of the armature reaction is applied in order to avoid the output power limitation.

III. CONTROL SYSTEM

The aim of the proposed power conditioning system is to supply the rated active power to the mains, and to compensate the reactive power and the current harmonics of non-linear loads. These requirements are met by generating sinusoidal source currents, in phase with the corresponding line-neutral source voltages. In order to achieve this result, two regulators are employed, one of them controls the DC-link voltage, while the other one determines the currents harmonics to be injected into the mains. The dynamic requirements for the two regulators are quite different. The AC current regulator must be designed in order to track the reference current waveforms closely, so this regulator must be much faster than the DC-link voltage regulator. As a consequence it is possible to treat the two regulators as decoupled loops [12].

A. DC-link voltage control loop

The basic principle of the DC-link voltage control loop is analyzed with reference to the block diagram of Fig. 2. In order to obtain a linear system, the energy stored in the DC-link capacitor ($E_c = 1/2 CV_{dc}^2$) has been considered as control variable, instead of the DC-link voltage V_{dc} . In this way, the transfer function representing the behavior of the DC-link

voltage control loop, can be determined [13]. The control strategy is based on the generation of a reference value for the source current space vector \bar{i}_S^* (having magnitude I_S^*), that is required to be in phase with the source voltage vector \bar{v}_S (having magnitude V_S). This is realized by the regulator $R(s)$ accepting the instantaneous value of the error signal, calculated as the difference of the actual and reference values of the energy stored in the DC-link capacitor.

The regulator output provides the reference value of the source active power P_S^* . According to the relationship $P_S^* = \frac{3}{2} V_S I_S^*$, the instantaneous value of \bar{i}_S^* is obtained multiplying P_S^* by the scaled value of the source voltage vector $\frac{2}{3} \frac{\bar{v}_S}{V_S^2}$, giving $\bar{i}_S^* = I_S^* \frac{\bar{v}_S}{V_S}$.

The dynamic behavior of the DC-link voltage control loop can be investigated with reference to the block diagram of Fig. 3. The reference value of the power supplied by the filter P_F^* , is calculated by adding the load power P_L to the reference source power P_S^* . Assuming an ideal PWM inverter, it yields $P_F = P_F^*$. This instantaneous power represents the total power flowing from the PCS to the mains, through the AC-link inductors. Neglecting the losses of the inductors and the change of the magnetic energy of the AC-link inductors in transient conditions, P_F can be also regarded as the output power of the VSI. Furthermore, neglecting the losses of the converter, the energy E_C stored in the DC-link capacitor can be expressed by the time integral of $(P_G - P_F)$, where P_G is the power supplied by the generator. Under these assumptions, the following equation can be derived

$$E_C = \frac{R(s)}{s + R(s)} E_C^* + \frac{1}{s + R(s)} (P_G - P_L). \quad (1)$$

As shown in (1), P_G and P_L can be considered as perturbation terms in the capacitor energy control loop. The effects of these perturbations are determined by the type of regulator, i.e. by the expression $R(s)$. The PCS has to supply the rated active power and compensate the current harmonics. Thus,

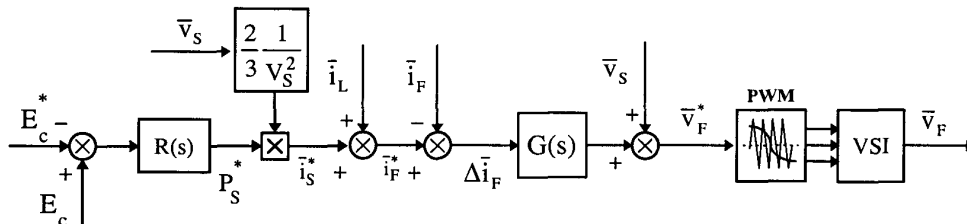


Fig. 2. Block diagram of the control system.

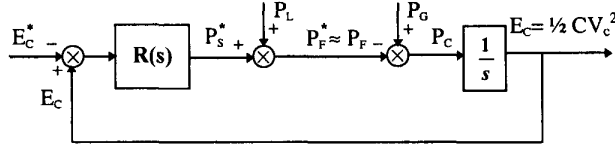


Fig. 3. Block diagram of the DC-link voltage control loop.

the design of the regulator $R(s)$ should be made by taking these requirements into account. It can be noted that, in general, good performance can be achieved using a PI regulator, thus $R(s)$ is described by the following expression

$$R(s) = K_p \frac{1 + T_i s}{T_i s}, \quad (2)$$

Substituting (2) in (1) yields

$$E_c = \frac{K_p s + K_p / T_i}{s^2 + K_p s + K_p / T_i} E_c^* + \frac{s}{s^2 + K_p s + K_p / T_i} (P_G - P_L). \quad (3)$$

It can be shown by (3) that, using a PI regulator, P_G and P_L do not introduce steady-state errors. Therefore, in response to load changes, the regulator acts to keep the reference value of the capacitor energy. With the same assumptions used in (1), the active power flowing to the source can be expressed as

$$P_S = \frac{R(s)}{s + R(s)} (P_G - P_L) - \frac{sR(s)}{s + R(s)} E_c^*. \quad (4)$$

It can be noticed that the relationship between $P_G - P_L$ and P_S is the same as between E_c^* and E_c in (1).

B. AC current control loop

The principle of operation of this control loop is analyzed with reference to the scheme shown in Fig. 2. The filter reference current \bar{i}_F^* is given by $\bar{i}_F^* = \bar{i}_S^* + \bar{i}_L$, where the load current is a measured quantity. If the losses of the AC-link inductors are neglected, the reference voltage \bar{v}_F^* for the PWM inverter can be calculated by the voltage equation of the AC-link inductance L , leading to

$$\bar{v}_F^* = \bar{v}_S + L \frac{\Delta \bar{i}_F}{\Delta t}, \quad (5)$$

where $\Delta \bar{i}_F = \bar{i}_F - \bar{i}_F^*$ is the filter current error accepted by the current controller $G(s)$.

The dynamic behavior can be investigated with reference to the block diagram of Fig. 4.

Assuming that the PWM inverter is able to generate the reference voltage at each cycle period ($\bar{v}_F = \bar{v}_F^*$), the following equation can be derived for the filter current

$$\bar{i}_F = \frac{1}{1 + \tau s} \bar{i}_F^*, \quad \text{where } \tau = L/K. \quad (6)$$

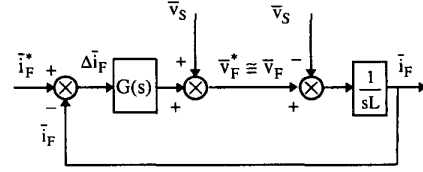


Fig. 4. Block diagram of the AC current control loop.

Eq. 6 has been obtained assuming for $G(s)$ a simple proportional gain K . In this case, the response of the AC current control loop can be represented by a first order low-pass filter. The dynamic behavior of the low-pass filter is mainly characterized by the inductance L , but its effect can be compensated choosing a suitable value for the gain K .

IV. CHARACTERISTICS OF THE TURBINE-GENERATOR SET

The mechanical characteristics of the turbine, at a given mass flow rate of the working medium, can be represented by

$$T_t = T_o - K_t \omega_m \quad (7)$$

where T_o is the turbine torque at zero speed and ω_m the mechanical angular speed. The constant K_t is set so as to obtain a torque of 20 Nm at the rated speed of 12000 rpm, corresponding to approximately 25 kW mechanical output power.

The generator is a 4-pole, permanent magnet, synchronous machine, with the following data

$$R_g = 0.114 \, \Omega, \quad L_g = 0.037 \, \text{H}, \quad K_g = 0.0357 \, \text{V/rad/s}.$$

The generator is connected to the three-phase diode rectifier through the synchronous impedance and a series capacitance C_g . The series capacitance has been introduced to compensate the voltage drop across the synchronous reactance and its value has been chosen to determine a series resonance at the rated frequency of 400 Hz, giving

$$C_g = 47.2 \, \mu\text{F}.$$

The DC-link capacitance is 4200 μF and the reference value of the DC-link voltage is 700 V.

The turbine-generator set connected to the rectifier has been numerically simulated by PSpice. The diodes have been represented by a default model which takes into account the power losses due to the forward voltage drop.

Fig. 5 shows the phase current and phase voltage waveforms of the generator when the rectifier is connected to a resistive load.

The effects of the series capacitance are represented in Fig. 6, where the DC-link voltage is plotted as function of the load current for different values of the angular frequency.

For a load current of 30 A (rated value) the DC-link voltage is 700 V and even with large variations of the load current the DC-link voltage shows small variations.

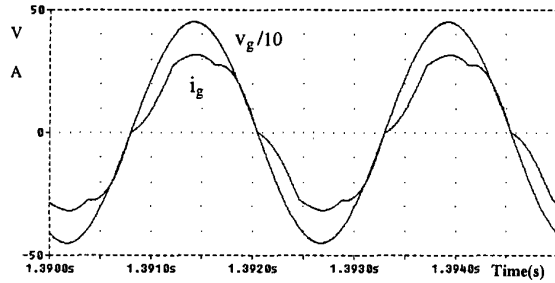


Fig. 5. Phase current and scaled phase voltage waveforms at rated speed.

V. NUMERICAL RESULTS

The complete system shown in Fig. 1 has been investigated by means of numerical simulations using PSpice. The inverter is connected to the 380 V, 50 Hz mains through three AC-link inductors having the following parameters

$$R = 0.1 \Omega, L = 0.0025 \text{ H.}$$

The semiconductor switches (IGBTs) of the inverter are controlled by a PWM technique based on a carrier frequency of 10 kHz. The analysis of the two control loops make it possible to determine the parameters of the regulators necessary to meet the dynamic requirements.

The numerical simulations have been carried out using the following gains for the DC-link voltage regulator: $K_p = 700$ and $K_I = K_p/T_i = 2$.

Various operating conditions have been studied in order to verify the capability of the system to behave as a power conditioner. First a three-phase linear load has been considered. The parameters of the load are $R_L = 7 \Omega$, $L_L = 0.013 \text{ H}$, corresponding to a load current of 27 A (RMS value) and a power factor of 0.866.

Figs. 7.1-7.3 show the dynamic behavior of the power conditioning system during the switching-on of the load. Due to the high inertia of the turbine-generator set, a small variation of the angular speed can be observed (less than 1 rad/s). The turbine speed returns to the reference value after nearly a second. With reference to DC-link voltage it can be evaluated the decrease at switching-on and the time necessary to recover the reference value. The control system takes about 30 ms to bring the DC-link voltage back to the steady state value (700 V).

Fig. 7.4 shows the current and source voltage waveforms in the steady-state operating conditions. It can be noted that the source current is in phase with the corresponding line-to-neutral source voltage.

Figs. 8.1-8.4 show the current and voltage waveforms during the load switching-off. The results obtained confirm that the control algorithm implemented and analyzed provides fast response in case of load changes. The cogeneration system is able to supply the rated active power with or without the load and to compensate the reactive power when the load is connected to the mains.

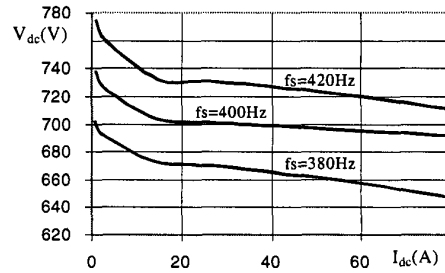


Fig. 6. Compensating effect of the series capacitance for different angular frequency values.

A three-phase full bridge rectifier has been considered to represent a non-linear load. The rectifier output is connected to an R-L load with $R = 20 \Omega$ and $L = 0.06 \text{ H}$.

The dynamic behavior of the angular speed during the switching-on and the switching-off of the non-linear load is quite similar to the one already discussed with a linear load.

In the case of non-linear load, the attention has been mainly focused on the capability of the power conditioning system to behave as an active filter. The dynamic behavior of the AC current control loop is determined by the gain of the proportional regulator K . The numerical simulation have been carried out using $K = 50$.

Figs. 9.1-9.3 illustrate the results obtained during the switching-on of the non-linear load. From Fig. 9.3, it is possible to verify that the PCS is able to compensate the load current harmonics. The source current has a sinusoidal waveform except for the high order harmonics caused by the fast current commutations of the diode bridge rectifier.

Figs. 10.1-10.3 illustrate the results obtained for the switching-off of the non-linear load. Following a switching-off of the load, the source current (which equals the filter current) is sinusoidal and in phase with the corresponding line-to-neutral source voltage.

VI. CONCLUSIONS

A novel control scheme for a cogeneration system has been presented and analyzed in this paper. The main feature of the proposed control method is its ability to operate the PCS as an active filter without modifying the power stages of the AC/AC converter. The control scheme is based on two independent control loops, one of them controls the DC-link voltage, setting the mechanical speed and the active power injected into the mains, while the other one ensures sinusoidal source currents with unity power factor. The performance of the system have been verified by numerical simulations (PSpice) in steady-state and transient operating conditions, using either linear or non-linear loads. The results obtained show that the behavior of the system as active filter is very good, the source currents are nearly sinusoidal, only a small distortion can be observed in the case high order load current harmonics.

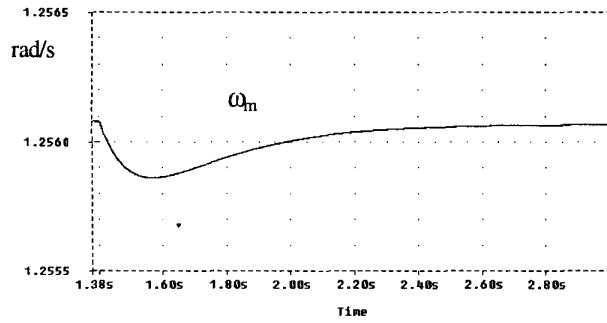


Fig. 7.1. Turbine speed variation during the load switching-on.

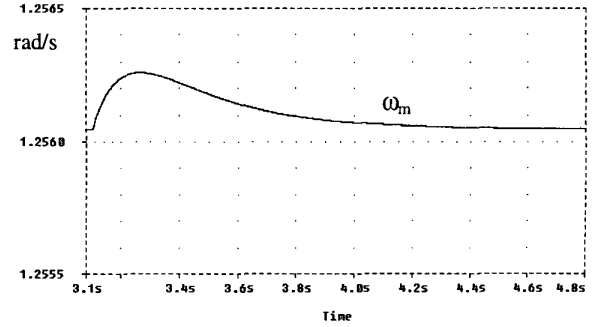


Fig. 8.1. Turbine speed variation during the load switching-off.

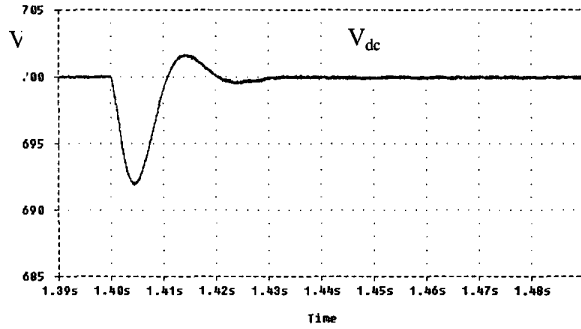


Fig. 7.2. DC-link voltage variation during the load switching-on.

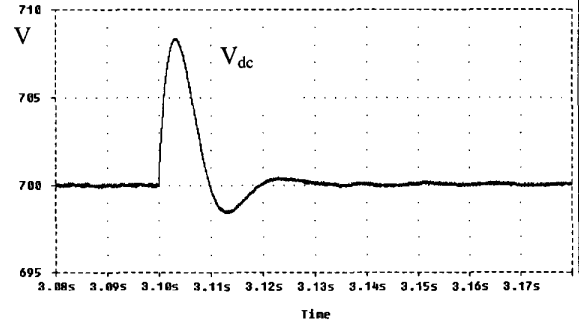


Fig. 8.2. DC-link voltage variation during the load switching-off.

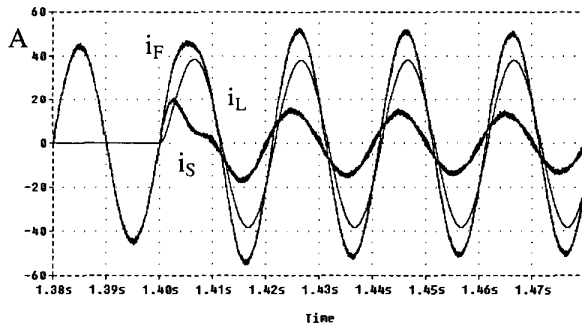


Fig. 7.3. Current waveforms during the load switching-on.

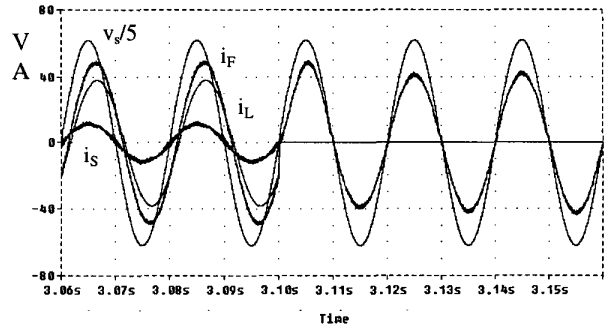


Fig. 8.3. Current and source voltage waveforms during the load switching-off.

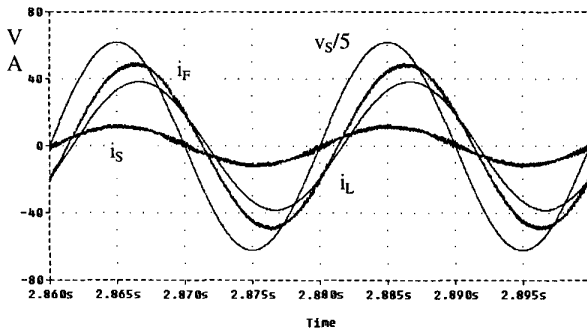


Fig. 7.4. Current and source voltage waveforms in steady-state operating conditions after the load switching-on.

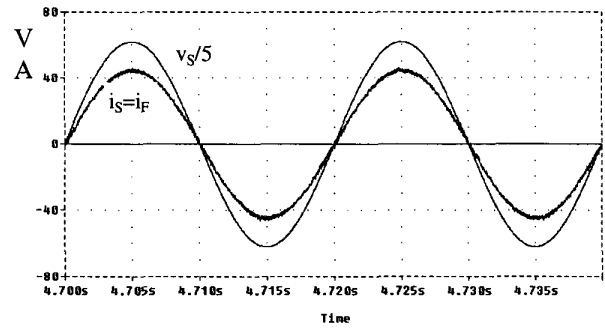


Fig. 8.4. Source current and source voltage waveforms in steady-state operating conditions after the load switching-off.

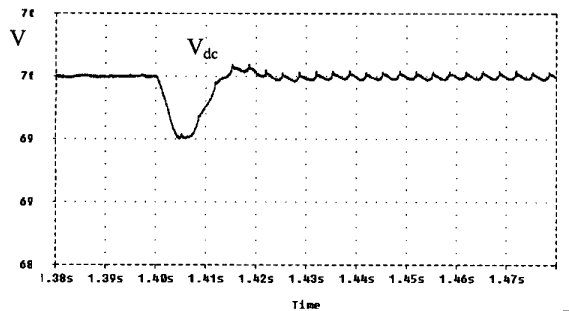


Fig.9.1. DC-link voltage variation during the load switching-on.

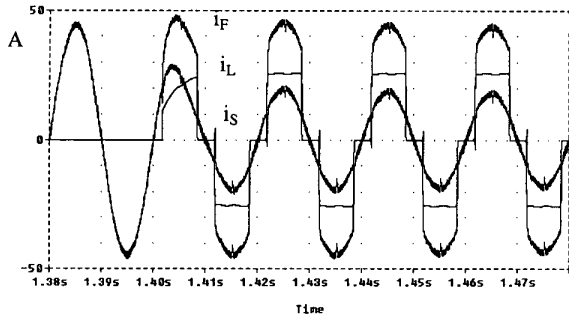


Fig.9.2. Current waveforms during the load switching-on.

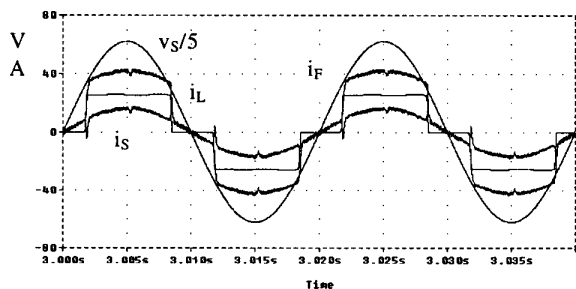


Fig.9.3. Current and source voltage waveforms in steady-state operating conditions after the load switching-on.

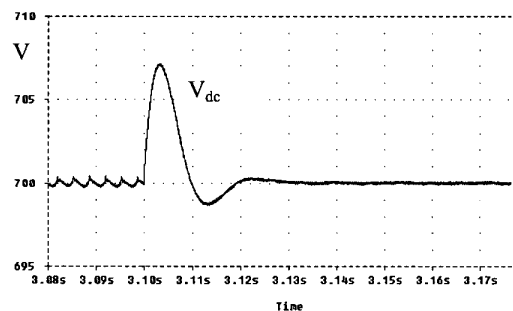


Fig.10.1. DC-link voltage variation during the load switching-off.

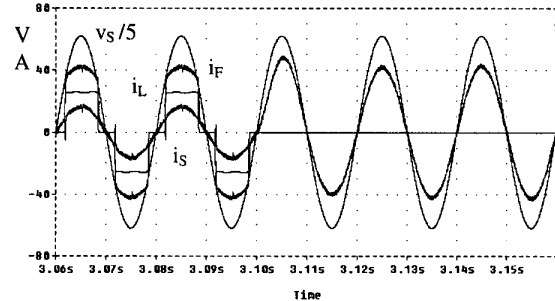


Fig.10.2. Current and source voltage waveforms during the load switching-off.

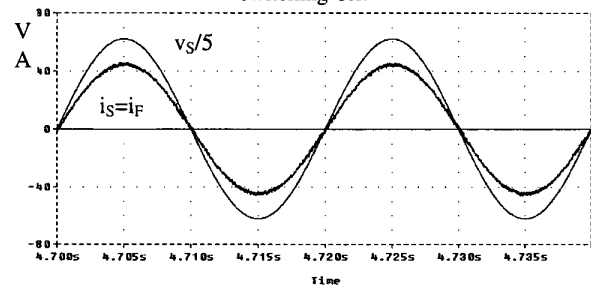


Fig.10.3. Source current and source voltage waveforms in steady-state operating conditions after the load switching-off.

REFERENCES

- [1] H.K. Lauw, J.B. Klaassens, N.G. Butler, D.B. Seely, "Variable-Speed Generation with Series-Resonant Converter," IEEE Transactions on Energy Conversion. Vol.3. No.4, Dec. 1988.
- [2] E. Raaijen, et. al. "An Efficient and Economical Active AC Line Conditioner," proceedings of Intelec'95 Conference October 29-November 1 1995. The Hague, The Netherlands.
- [3] R.K. Jordan, "Generation of Electric Energy by High-Speed Turbine - Generator Sets," proceedings of Intelec'95 Conference October 29-November 1. The Hague, The Netherlands.
- [4] L. Gyugyi, E.C. Strycula, "Active AC Power Filter," Proc. IEEE-IAS Annual Meeting, pp. 529, 1976.
- [5] H. Akagi, Y. Kanazawa, A. Nabae, "Instantaneous Reactive Power Compensators Comprising Switching Devices without Energy Storage Components," IEEE Transactions on Industry Applications, Vol. 20, 1984.
- [6] L. Malesani, L. Rossetto, P. Tenti, "Active Filters for Reactive Power and Harmonic Compensation," Proc. IEEE-PESC, pp. 321-330, June 1986.
- [7] H. Fujita, H. Akagi, "The Unified Power Quality Conditioner: The Integration of Series Active Filter and Shunt Active Filters," Proc. IEEE-PESC, Baveno (IT), pp. 494-501, June 1996.
- [8] S. Bhattacharya, D.M. Divan, "Design and Implementation of a Hybrid Series Active Filter System," Proc. IEEE-PESC, Atlanta, 1995.
- [9] V. Soares, P. Verdelho, G. Marques, "Active Power Filters Control Circuit Based on the Instantaneous Active and Reactive Current i_d - i_q Method," Proc. IEEE-PESC, pp. 1096-1108, June 1997.
- [10] P. Delarue, R. Bausierre, "New Control Methods for Active Power Filter Needing Line Current Measurements only," Proc. EPE, Sevilla (SP), Vol. 1, pp. 914-919, 1995.
- [11] L.A. Moran, J.W. Dixon, R.R. Wallace, "A three phase active power filter operating with fixed switching frequency for reactive power and current harmonic compensation," IEEE Transactions on Industrial Electronics, Vol. 42, No.4, pp.402-408, 1996.
- [12] D. Casadei, U. Reggiani, G. Grandi, "Active power filters based on a single current measurement system," Proceedings of SPEEDAM, Sorrento, Italy, pp. B3.19-B3.23, June 3-5, 1998.
- [13] D. Casadei, G. Grandi, U. Reggiani, G. Serra, "Analysis of a Power Conditioning System for Superconductive Magnetic Energy Storage (SMES)," Proc. IEEE-ISIE Pretoria (SA), Vol.2, pp.546-551, July, 1998.